Contents lists available at SciOpen

Food Science and Human Wellness

journal homepage: https://www.sciopen.com/journal/2097-0765

China Food Publishing Co.

Chronic and acute acrylamide exposure on cell-type-specific neurotoxicity in bumblebee brain

Peijiong Wang[a], Qiyao Yong[b], Huiling Liu[b], Xiaohuan Mu[b], Xiaofei Wang[b], Fang Chen[b], Hao Zheng[b,*] Yiyuan Li[c,*]

[a] *Department of Neurosurgery, The First Affiliated Hospital of Zhengzhou University, Zhengzhou 450052, China*
[b] *National Engineering Technology Research Center for Fruit and Vegetable Processing, Key Open Laboratory of Fruit and Vegetable Processing, Ministry of Agriculture and Rural Affairs, Beijing Key Laboratory of Food Non-thermal Processing, College of Food Science and Nutritional Engineering, China Agricultural University, Beijing 100083, China*
[c] *Department of Gastroenterology, The First Affiliated Hospital of Zhengzhou University, Zhengzhou 450052, China*

ARTICLE INFO

Article history:
Received 13 August 2024
Received in revised form 26 August 2024
Accepted 26 December 2024

Keywords:
Acrylamide
Neurotoxicity
Bombus terrestris
Single-nucleus RNA sequencing
Kenyon cell
Glia

ABSTRACT

Acrylamide (AA) is a common carcinogen that affects the development and function of the central nervous system (CNS). At present, the toxic injuries of common AA are mainly divided into acute and chronic attacks, and the damage caused to the CNS is different. To investigate whether different doses of AA have different effects on brain cells, we performed single-nucleus RNA sequencing of the brain. The findings indicated that short-term high-dose (acute) AA directly disrupted protein synthesis and protein structure stability on the endoplasmic reticulum. Additionally, acute AA was observed to downregulate genes that inhibit apoptosis and autophagy, promote apoptosis, accelerate cell aging, and affect cell function in glial cells (Glia). Long-term low-dose (chronic) AA exposure elevated Ca^{2+} concentration, increased protein autophosphorylation, and induced mitochondrial dysfunction, resulting in impaired axonal transport and disrupted metabolism of Kenyon cells (KCs). These findings highlight the cell type-specific effects of AA, where acute exposure disrupts Glia protein homeostasis, and chronic exposure impairs calcium signaling and axonal transport in KCs. Such results deepen our understanding of AA-induced neurotoxicity and lay the groundwork for developing targeted therapeutic strategies to mitigate its effects on the CNS.

1. Introduction

Acrylamide (AA), a water soluble vinyl monomer, is mainly used in the synthesis of polyacrylamides employed in the industry applications for wastewater treatment, soil conditioning, textile, and paper production[1]. Additionally, AA can largely be generated in foods cooked at high temperatures, primarily through the Maillard reaction[2-3], and more than one-third of the calories consumed by U.S. and European populations derived from foods containing AA[4]. Exposure to AA through ingestion, dermal contact, or inhalation can lead to various harmful effects, including developmental issues[5-6], reproductive toxicity[7-8], and neurotoxicity[1,9]. In consideration of the carcinogenic and genotoxic properties of AA, the International Agency for Research on Cancer has designated AA as a Class 2A substance[10-12].

The neurotoxic effects of AA were first recognized in the 1950s, subsequent research has shown a marked increase in the incidence of neurotoxicity among these populations over time[13-14]. In cases of acute AA poisoning, especially under high exposure levels (approximately 400 mg/L via well water), the central nervous system (CNS) is the primary target[15]. Furthermore, in occupational environments with low-dose and prolonged exposure, symptoms of

* Corresponding authors.
E-mail address: hao.zheng@cau.edu.cn (H. Zheng); lyyattth@163.com (Y.Y. Li)
Peer review under responsibility of Beijing Academy of Food Sciences.

SciOpen Publishing services by Tsinghua University Press

http://doi.org/10.26599/FSHW.2024.9250457

peripheral nerve dysfunction become apparent[16]. Despite extensive research on the molecular mechanisms underlying its neurotoxicity, the existing literatures have predominantly focused on the collective response of cell populations, leaving cell-specific changes relatively ambiguous.

The brain, arguably the most intricate organ, comprises a diverse array of cell types, including neurons and glial cells (Glia), as well as various subtypes derived from these cells[17]. The multiplicity of brain cell types, as well as their intricate connectivity, presents formidable challenges to understanding AA-induced neurotoxicity. Recent studies in rats and human cell models have found that the neurotoxic response to AA is neuron-type specific[1]. Therefore, it is important to investigate whether the cell-type heterogeneity of AA effects corresponds to distinct functional specialization at the single-cell level. Single-nucleus RNA sequencing (snRNA-seq) emerges as a valuable tool for addressing this challenge[18-22], to pinpoint the specific cell types targeted by AA and elucidate the transcriptome heterogeneity that exists among these cell types.

While neurotoxicity testing on animals has traditionally been a fundamental part of non-clinical laboratory evaluation, the ethical concerns associated with the use of mammals such as primates, rodents, or dogs have garnered widespread attention[23]. As an alternative approach, *in vivo*, methods using non-rodent models have emerged as innovative platforms for high-throughput screening of the neurotoxic effects, such as the zebrafish (*Danio rerio*)[24-25], *Drosophila melanogaster*[6] and *Caenorhabditis elegans*[26]. Among these non-traditional model organisms, the bumblebee (*Bombus terrestris*) stands out as a remarkably well-studied insect species with an impressive range of cognitive abilities, including olfactory learning, color discrimination, and even object manipulation with specific targets[27-29]. Furthermore, bumblebee has a potential to serve as a viable model for the study of neurodegenerative diseases. Chen et al.[30] have identified numerous differentially expressed genes (DEGs) in the brains of rotenone-treated bumblebees that overlap with Parkinson's-related genes. Additionally, immunofluorescent staining has also demonstrated that rotenone induces apoptosis in dopamine neurons, a process that is similar to that observed in human Parkinson's disease. In conclusion, the relatively small and simple structure of the bumblebee brain, combined with the observed parallels between the behavioral and gene expression patterns in bumblebees and humans, provides researchers with a valuable model for investigating the effects of neurotoxic substances on the brain.

In this study, we investigated the neurotoxic effects of AA on behavioral phenotypes and identified the molecular and cellular targets underlying both its acute and chronic actions, utilizing bumblebees as a model organism. Behavioral results revealed that both acute and chronic AA exposure increased locomotion and impaired cognitive ability in bumblebees. To better elucidate the cell-type specific responses to AA-induced neurotoxicity, we employed snRNA-seq to construct a transcriptome atlas containing all major brain cell types, including neurons and Glia, along with their subpopulations. By comparing relative cell-type abundance and gene expression profiles across exposure conditions, our study sought to identify cellular pathways and biological processes that may be differentially affected by acute and chronic AA exposure, thereby providing mechanistic insights into AA-induced neurotoxicity.

2. Materials and methods

2.1 Animals

The bumblebees (*B. terrestris*) used in this study were obtained from Shandong Academy of Agricultural Sciences and Beekeeping Breeding Base ((Lu)AQ101751, Yantai, China). The bumblebee colonies were reared in a plastic box (17 cm × 11.5 cm × 6.7 cm) with 50% (*m*/*m*) sucrose solution and kept in incubators at 65% humidity and 29 °C. After one day of incubation, callow workers with a chest width of (5.0 ± 0.5) mm were selected and placed in groups of 3 in a dwarf cup. They were then fed with different concentrations of AA solution or sucrose solution. During the experiment, fresh pollen was provided ad libitum, and bumblebees kindly after the experiment.

2.2 Bumblebees rearing and AA exposure

AA was obtained from BioDee Biotechnology Co., Ltd. (Beijing, China). Bumblebees were fed AA solutions (prepared with sterile sucrose solution with a mass fraction of 50%) at concentrations of 2, 1, 0.5, 0.1, and 0 mmol/L for 10 days, and mortality and body weight were recorded. Mortality curves were plotted based on the mortality of bumblebees, and the concentration close to the control mortality was selected as the acute and chronic concentration. Prior to the administration of AA, the initial body weight of each bumblebee was determined using a balance. Following a 2-day acute AA treatment and a 5-day chronic AA treatment, the body weights of the corresponding groups of bumblebees were weighed. The rate of change in body weight was calculated as the difference between the treated body weight and the initial body weight, divided by the initial body weight.

2.3 Locomotion assay

The bumblebee motility was measured by the behavioral software EthoVision XT 17 (Noldus, Wageningen, Netherlands). The bumblebees were individually transferred to 90 mm petri dishes and placed in a well-lit room at 26 ℃. After a 30-min acclimation, we recorded continuous 30-min videos to monitor each bumblebee's movements. Subsequently, the videos were imported into EthoVision XT 17 software to delineate the movement area and the bees' movement data were recorded. The distance, velocity, maximum deceleration, and acceleration during the video time were analyzed.

2.4 Learning and memory assay

We measured the learning and memory abilities of bumblebees after being subjected to acute and chronic doses of AA. Prior to the learning and memory assay, pollen and sucrose solution were removed for 2-h starvation. Then, they were fixed using tape in 2 mL centrifuge tubes with slits cut out. The entire learning and memory experiment was conducted in a room with a stable light source at 26 ℃. Before the experiment, the proboscis extension response (PER) of each bumblebee was tested by touching the antennae with a 50% sucrose solution. Bumblebees that did

not exhibit a PER were removed from further experiments. A filter paper was placed in a 10 mL syringe, and 0.5 mL of lemon essential oil (Phutawan, Thailand) was injected into the filter paper as the odor source. Air served as the negative control.

Before the start of each trial, the bumblebees were left in the experimental site for 10 s to familiarise themselves with the experimental background. Then, bumblebees were provided with clean air for 5 s, followed by lemon odor for 10 s. At 6 s, a 50% sucrose solution was used to stimulate the bumblebees to induce the PER. Bumblebees were trained once every 10 min for a total of 10 rounds. During training, bumblebees that extended their proboscis were rewarded with a 50% sucrose solution to form a conditioned reflex. Bumblebees were considered to have good learning ability if they extended their proboscis solely in response to the lemon stimulus. Three hours after the learning test, the bumblebees' memory capacity was evaluated by retesting them with lemon odor and recording their showed a PER.

2.5 Brain collection, single-nucleus suspension preparation, and snRNA-seq determination

Bumblebee brains were collected with a dissecting microscope (SMZ745T, Nikon, Japan). The thorax was passed through 2 insect pins and fixed on a wax disc. The bumblebee's head cuticle was incised, and the brain was carefully extracted with forceps, placed on a slide, and followed by the removal of the hypopharyngeal glands, salivary glands, three single eyes, and two compound eyes. The whole brain was rapidly frozen in liquid nitrogen and kept frozen at -80 °C until analysis.

We used DNBelab C Series Single-Cell Library Prep Set (MGI, 1000021082) based on droplet microfluidic technology for library construction, pooling 1 000 nuclei/μL per library concentration for library preparation. First, the single nuclear suspensions were converted into a barcoded snRNA-seq library by droplet encapsulation, emulsion fragmentation, mRNA capture bead acquisition, reverse transcription, cDNA amplification, and purification. Then, the Qubit ssDNA Assay Kit (Thermo Fisher Scientific, Q10212) was built and quantitatively indexed to sequence the library. The snRNA libraries were then sequenced using the DIPSEQ T1 platform at the National Gene Bank of China (Shenzhen, China) and the following sequencing strategies were employed. Read length of 41 bp for Read 1 and 100 bp for Read 2.

Raw data obtained by snRNA-seq on the DNBSEQ-T1 platform were filtered and demultiplexed using PISA v0.2 (https://github.com/shiquan/PISA). Compare the reads with the reference genome of *B. terrestris* (GCA_910591885.2 iyBomTerr1.2_genomic) using STAR (v2.5.1b) (https://github.com/alexdobin/STAR)[31] and perform downstream calculations using sambamba (version 0.7.0)[32]. These reads were annotated with "PISA anno" according to the gene transfer format file of the *B. terrestris* genome. According to the cut-off point between empty and non-empty barcodes in SoupX (v1.4.8)[33], the barcode rank plots were generated and the noise of ambient RNA was reduced. The matrix of cell versus gene unique molecular identifiers (UMI) counts was generated using PISA.

2.6 Downstream analysis of snRNA-seq data

2.6.1 Quality control, integration, feature selection and dimensionality reduction

The Seurat (v4.0.5) package was executed on each library. Cells classified on nFeature RNA (number of genes expressed in a cell) and 5th to 95th percentile were retained, and each gene was detected in at least three cells. Cells with high mitochondrial content (UMIs were classified with a percentage of 0.03 mitochondrial genes) were dropped. For each library, we used DoubletFinder (v2.0) to remove potential double cells. It is estimated that the expected bimodal rate was 5%, the number of artificial bimodals was set to 0.25 and the neighborhood size pK was set to 0.01 to generate pseudo-bimodal. According to the order of the distribution of the artificial proportion of nearest neighbor (pANN), cells with the highest pANN value (> pK) were predicted to be doublets. The UMI count matrix was normalized by the 'NormalizeData', and the mean-variance relationship was controlled by the 'FindVariableFeatures' to select the most variable genes. The Seurat function of 'RunPCA' was used to calculate the principal components (PCs).

Using the 'FindIntegrationAnchors' and 'IntegrateData' functions, all libraries were integrated into a matrix containing the top 30 PCs. The following parameters were applied to correct for batch effect in sequencing: reduction of 'rpca', and normalization method 'LogNormalize'. The synthetic expression values were then scaled using the 'ScaleData' function and PCs were calculated using 'RunPCA' for the first 2 000 variable genes.

2.6.2 Cluster analysis and cell type annotation

Firstly, we performed graph-based unsupervised clustering with 'FindNeighbors' and 'FindClusters' with different resolution parameters (0.2, 0.5, 0.8, 1.2, 1.6), and then a clustering tree using the R package clustree (v0.4.3) to visualize the relationship between multiple resolutions. Finally, select the appropriate resolution for subsequent analysis. Next, to identify cell types in the bumblebee brain, we primarily annotate cells by examining the expression patterns of marker genes previously defined in *Apis mellifera*[34], *D. melanogaster*[35], *Harpegnathos saltator*[36] and *Monomorium pharaonic*[37]. To determine the homologous genes among *B. terrestris* and these insects, we referred to the orthogonal gene provided by OrthoDB (v10.1) database, and protein sequences with 2-way reciprocal best hits identified by Diamond (v0.8.23) (*e*-value < 1×10^{-5}, percentage of identical matches > 30%). Cell clusters were annotated for cell types based on the percentage of UMIs corresponding to marker genes within each cluster.

2.6.3 Differential expression analysis

We performed DEG analysis in different cell clusters. To identify DEGs in each cluster, the Seurat function 'FindMarkers' was used to find genes that were more highly expressed in each cluster relative to those in other clusters. We determined DEGs between two groups of cells using the Wilcoxon rank sum test, with differences quantified by the $\log_2$ fold change ($\log_2$ FC) metric. Significant DEGs were determined using thresholds of $|\log_2 FC| > 0.5$ and $P < 0.05$ and were visualized using

the EnhancedVolcano (v1.13.2) and ggplot2 (v3.3.6) package. Then, Gene Set Enrichment Analysis (GSEA) for DEGs in each cell type was conducted on the Kyoto Encyclopedia of Genes and Genomes (KEGG) pathway using the ClusterProfiler package (v4.2.2).

2.7 RNA extraction, cDNA synthesis, and quantitative real-time polymerase chain reaction (qPCR)

Bumblebee brains were dissected according to the protocol outlined in Section 2.5, and subsequently placed into clean 1.5 mL centrifuge tubes. The tissues were homogenized using a tissue grinder (TIANGEN, Beijing, China), and total RNA was extracted following the manufacturer's instructions for the RNA-easy Isolation Reagent (R701-01; Vazyme, Nanjing, China). A HiScript III All-in-one RT SuperMix Perfect for qPCR (R333-01; Vazyme, Nanjing, China) was used to synthesize cDNA. qPCR was performed using a QuantStudio 1 Real-Time PCR instrument (Thermo Fisher Scientific, Waltham, Massachusetts) using Tag Pro UniversalSYBR qPCR Master Mix (Q712; Vazyme, Nanjing, China). Data analysis was performed using the $2^{-\Delta\Delta Ct}$ method and the sequences of the qPCR primers are provided in Table S1.

3. Results and discussion

3.1 Acute and chronic AA exposure induced locomotor deficits and cognition impairment

In order to determine acute and chronic AA treatment for subsequent investigation, four concentrations of AA (0.1, 0.5, 1, and 2 mmol/L) were employed, toxicologically equivalents relevant to human exposure in values of approximately 15.8, 79, 158, and 316 mg/(kg·day). The mortality curve revealed that 2 mmol/L AA led to the demise of all bumblebees within one week, while no significant difference was observed during the initial 2 days (Fig. S1A). Body weight measurements revealed no significant changes across the different acute and chronic exposure groups (Figs. S1B-C). Previous studies demonstrated that median lethal concentration (LC_{50}) was approximately 2 mmol/L in zebrafish[38] and *D. melanogaster*[6], while the oral lethal dose levels of AA were stated among 107–250 mg/kg in rats, guinea pigs, mice and other mammalian animals[39], and oral concentrations exceeding 100 mg/(kg·day) exhibit significant acute toxicity[40]. The 0.1 mmol/L AA treatment maintained a similar survival rate to that of the control group, with no mortality observed throughout the experiment (Fig. S1A), paralleling findings in *D. melanogaster*[6]. Consequently, we established an acute AA exposure as short-term high-dose concentration of 2 mmol/L for 2 days, and a chronic AA exposure as long-term low-dose concentration of 0.1 mmol/L for 5 days.

To investigate the effects of AA on bumblebee behavior, we first assessed the bumblebees' locomotion and cognition (Fig. 1A). The video recordings capturing bumblebee movements showed that acute AA exposure significantly compromised their locomotor capabilities, across all 5 parameters: trajectory, distance, velocity, maximum deceleration and acceleration. Compared to the control, bumblebees exposed to acute AA exhibited a circular motion along the perimeter of the petri dish (Fig. 1B), indicating symptoms of anxiety. The change in locomotor behavior of bumblebees exposed to acute AA mirrors the anxiety-related symptoms observed in zebrafish, which exposed to 0.75 mmol/L AA tended to remain at the periphery of the open field rather than the central area, showing reduced exploratory behavior[41]. Additionally, they were less likely to enter the open arm of the elevated cross maze and spent less time in the bright chamber of the dark-light box test[42-43]. After acute AA treatment, the movement distance, velocity, and maximum acceleration of bumblebees decreased by 40.4%, 40.2%, and 46.2%, respectively, which were significant differences compared to the control group (Fig. 1C). Similarly, zebrafish exhibited a reduction in total distance traveled and movement time in both open field and novel tank tests[41]. In humans and mammals[44], AA neurotoxicity is also characterized by impaired motor function, consistent with the results observed in bumblebees. To elucidate the effects of AA on cognitive ability, we conducted the olfactory learning and memory experiment, a reliable example of cognition ability in insects. After the acute AA treatment, bumblebees exhibited PER during the second round of lemon odor stimulation. With successive test rounds, the learning rate of the bumblebees increased gradually before stabilizing at 36.67%, which was significantly lower than the control group's 62.16% (Figs. 1D-E). Correspondingly, rats exposed to 100 mg/L AA took longer to find the hidden platform[45], and a worker accidentally exposed to a large amount of AA developed slurred speech and memory impairment[46].

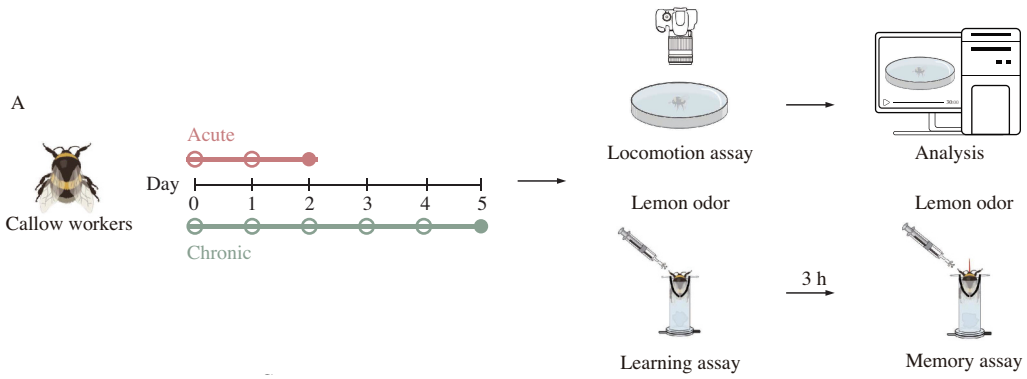

Fig. 1 Effects of chronic and acute AA on the behavioral activity of bumblebees. (A) Flow chart diagram of the bumblebee behavior test in the present study. (B-C) The changes in trajectory, distance, velocity, maximum deceleration, and acceleration of bumblebees after acute AA exposure. Effects of acute AA exposure on learning (D) and memory (E) in bumblebees. (F-G) The changes in trajectory, distance, velocity, maximum deceleration, and acceleration of bumblebees after chronic AA exposure.Effects of chronic AA exposure on learning (H) and memory (I) in bumblebees. Significant differences from the control are indicated by * $P < 0.05$, ** $P < 0.01$.

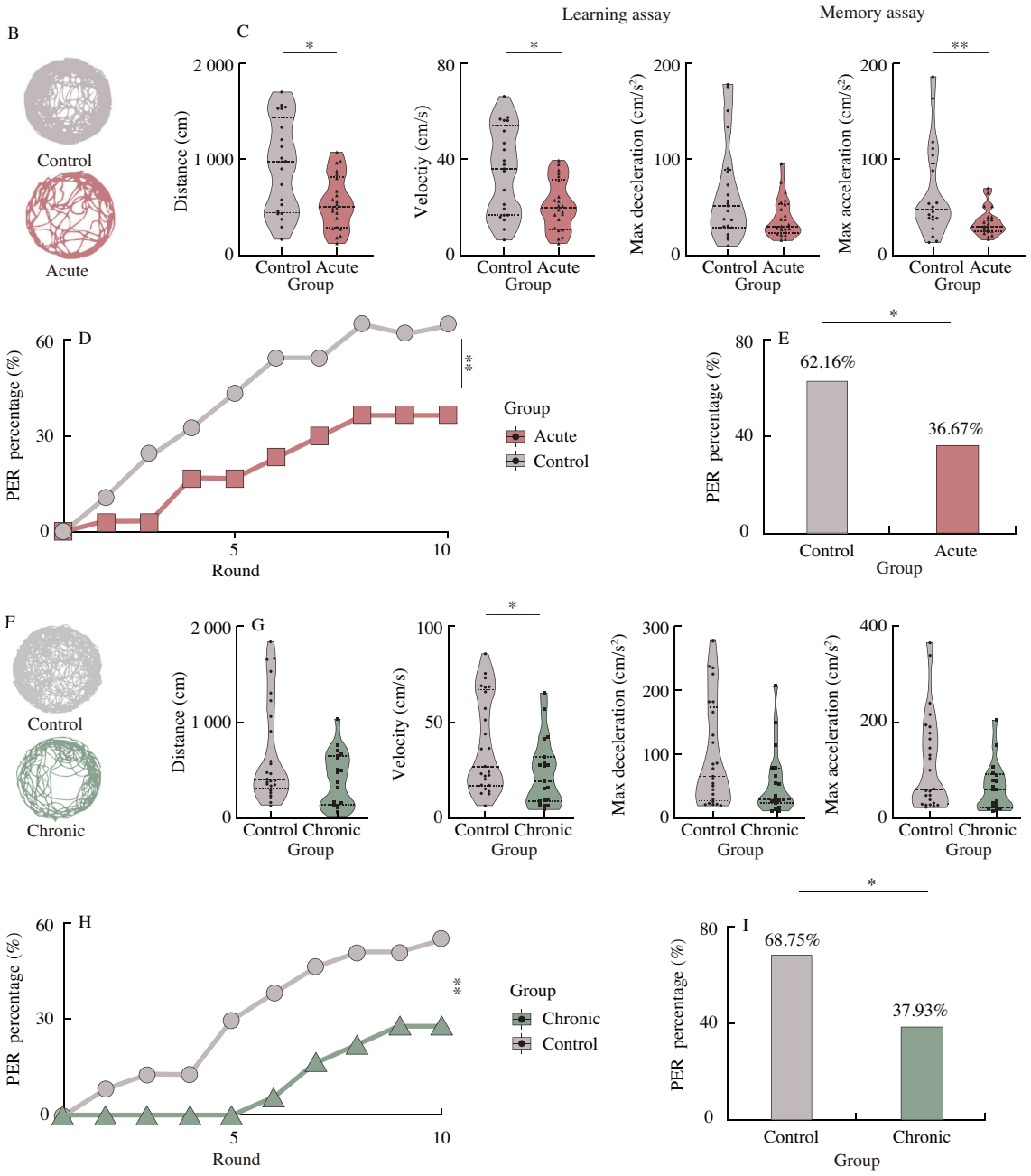

Fig. 1 (*Continued*)

Similarly, prolonged ingestion of low-dose AA resulted in significant impairments in both motor and cognitive abilities. In contrast to the acute AA treatment, bumblebees treated with chronic AA tended to crawl along the edge of the test area and demonstrated impaired motor function, as evidenced by decreased crawling velocity (Figs. 1F-G). Correspondingly, chronic AA exposure also resulted in decreased velocity in zebrafish and abnormal gait in rats[47-48]. Additionally, long-term AA exposure significantly impaired the cognitive abilities of bumblebees, with only 37.93% exhibiting good learning and memory abilities compared to 68.75% in the control (Figs. 1H-I). Interestingly, bumblebees treated with chronic AA exhibited a PER to lemon odors only by the 6th learning round (Fig. 1H), significantly later than those treated with acute AA (Fig. 1B). Studies have demonstrated that rats experience cognitive impairment following chronic AA treatment[49]. Similarly, epidemiological research indicates that workers with an average dietary intake of 57 mg/day of AA exhibit decreased cognitive abilities in neuropsychological function tests[50]. Evidence suggests that gene expression is closely linked to behavior, with changes in brain gene expression mediating behavioral changes. This relationship between specific genes and behavior has been observed to persist across various timescales[51]. Although the neurotoxic hazard and risks of AA exposure have been extensively reported in other model animals, the specific mechanisms by which AA causes neurotoxicity remain unclear.

3.2 AA exposure induced cell-specific responses

To investigate the causes of these behavioral changes in the brains across different cell types, we performed snRNA-seq on control and AA-treated bumblebees to elucidate the specific mechanisms of AA's effects on the brain at the single-cell level. Upon the completion of the sequencing and quality control processes, a total of 13 libraries were obtained, comprising 77 554 nuclei. To exclude batch effects of libraries and treatments, we integrated the control and AA-treated data and classified these cells into 28 distinct clusters using a resolution parameter of 0.2 (Fig. 2A). Subsequently, we employed *t*-distributed stochastic neighbor embedding (*t*-SNE) for global visualization, which revealed that the clustering outcomes following AA treatment were analogous to those of the control group (Fig. 2B). Based on the expression of known marker genes, the 28 clusters were manually annotated into four major cell types: Glia, KCs, optic lobe cells (OLCs), and olfactory projection neurons (OPNs). Specifically, ten were identified as Glia, expressing markers such as *Gs2*, *Galphai*, *gem*, *Gat*, *Eaat1*, and *Tsf1*; three were designated as KCs, characterized by *PLCe*, *Camkii*, *Dop1R2*, and *Pka-C1*; six were classified as OLCs, marked by *hbn*, *ort*, and *CG8916*; while one was defined as OPNs, distinguished by *Drgx*[34-37] (Fig. 2C).

Subsequently, we quantified the relative abundance of distinct cell types. The analysis demonstrated that Glia and KCs constituted the predominant cell populations, accounting for 36.1% and 30.5% of the total cells, respectively (Figs. 2D-G). Interestingly, the proportion of KCs decreased significantly after chronic and acute AA treatment, whereas the proportion of Glia increased significantly (Figs. 2D-E). Furthermore, we focus on DEGs in each cell type between control and AA treatment. After acute AA exposure, 543 DEGs were identified, excluding unknown data, the number of DEGs in Glia, KCs, OLCs, and OPNs were 111, 87, 137, and 136, respectively (Figs. S2A-B). In contrast, the chronic AA exposure group yielded a total of 1 817 DEGs. Among these, 302 DEGs were identified in Glia, 365 in KCs, 401 in OLCs, and 387 in OPNs (Figs. S2C-D).

The data reveal notable discrepancies in how distinct cell types react to AA, likely due to their specific functions and varying sensitivities within the CNS. Further KEGG analysis revealed that both acute and chronic AA exposures led to the activation of signaling pathways that are closely associated with neurodevelopment and motor metabolism. Specifically, acute AA exhibited a different pattern of pathway regulation, with inhibition of endoplasmic reticulum protein processing and synthesis, especially prominent in Glia (Fig. 2H). Correspondingly, Schotman et al.[52] demonstrated that the protein synthesis rate in rats was inhibited following AA poisoning, which was analogous to the alterations in tracer leucine incorporation observed in previous experiments[53]. Glia are the primary regulators of cell number within the CNS, which have the capacity to affect several processes, including neuronal migration, axonal specialization and growth, and the regulation of synaptic communication, plasticity, and brain metabolism[54]. Consequently, impaired Glia function may have a negative impact on the overall health of the CNS. In contrast, chronic AA appeared to induce neuronal damage by modulating calcium signaling pathways and axonal transport-related pathways (Fig. 2I). Studies have demonstrated that nerve endings are the primary target of AA, and the neurotoxicity of AA is cumulative, eventually predisposing to axonal degeneration with increasing exposure time[1,55]. Furthermore, AA was also inducing Ca^{2+} disruption and ATP depletion in cytosolic SH-SY5Y cells, corresponding to our enrichment results[56]. Notably, these pathways were most evidently altered in KCs (Fig. 2I). As cells that play a critical role in neurodevelopment and cognitive behavior, the impaired function of KCs is consistent with our behavioral findings of motor and cognitive impairments[57].

Overall, our findings suggested that AA exposure can have cell-specific responses, with chronic exposure primarily affecting neurodevelopment-related pathways in KCs and acute exposure leading to disruptions in protein processing and synthesis pathways in Glia, ultimately impacting their cellular functions.

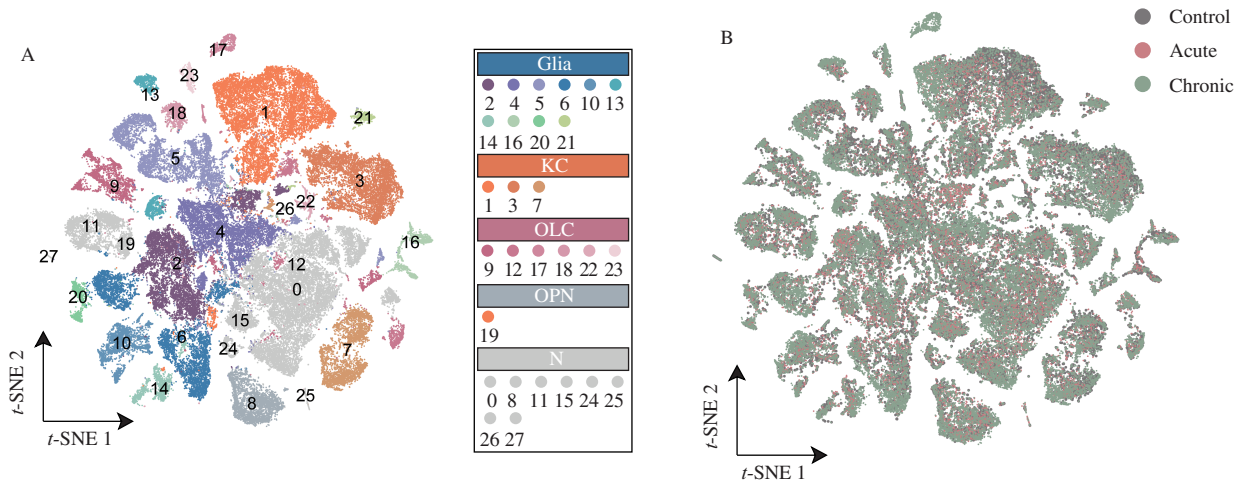

Fig. 2 Single-cell transcriptional atlas and the effects of AA on the bumblebee brain. (A) Single-cell transcriptional atlas of the bumblebee brain. (B) Impact of AA treatment on the clustering of brain cells. (C) Expression profiles of brain cell type-specific marker genes across distinct clusters. Glia: cluster 2, 4, 5, 6, 10, 13, 14, 16, 20, 21; KC: cluster 1, 3, 7; OLC: cluster 9, 12, 17, 18, 22, 23; OPN: cluster 19. Relative proportions of Glia (D), KCs (E), OLCs (F), and OPNs (G) across control, acute, and chronic AA treatment groups. (I) Up-regulation of pathways following chronic AA exposure. Different letters indicate significant differences ($P < 0.05$).

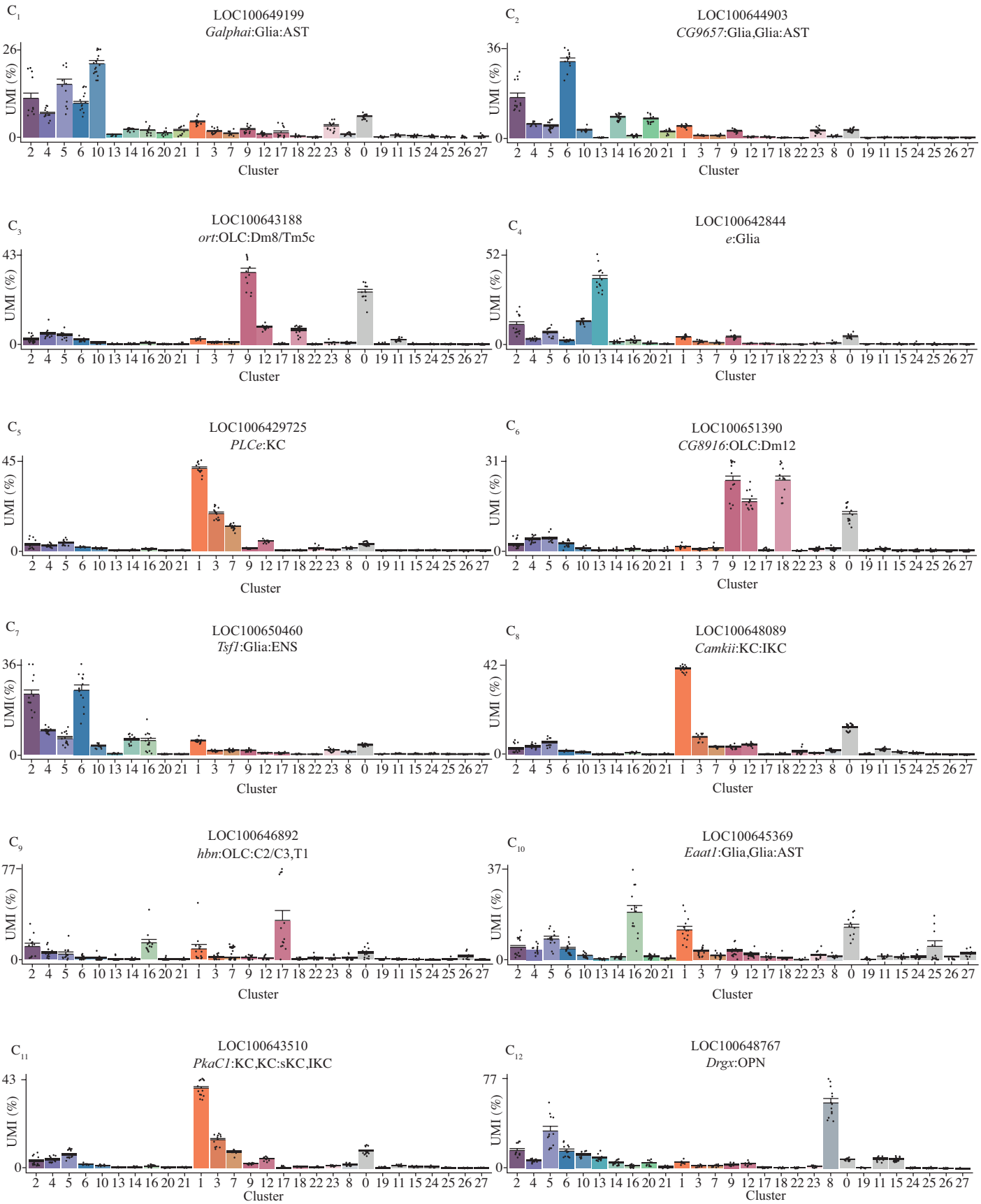

Fig. 2 (*Continued*)

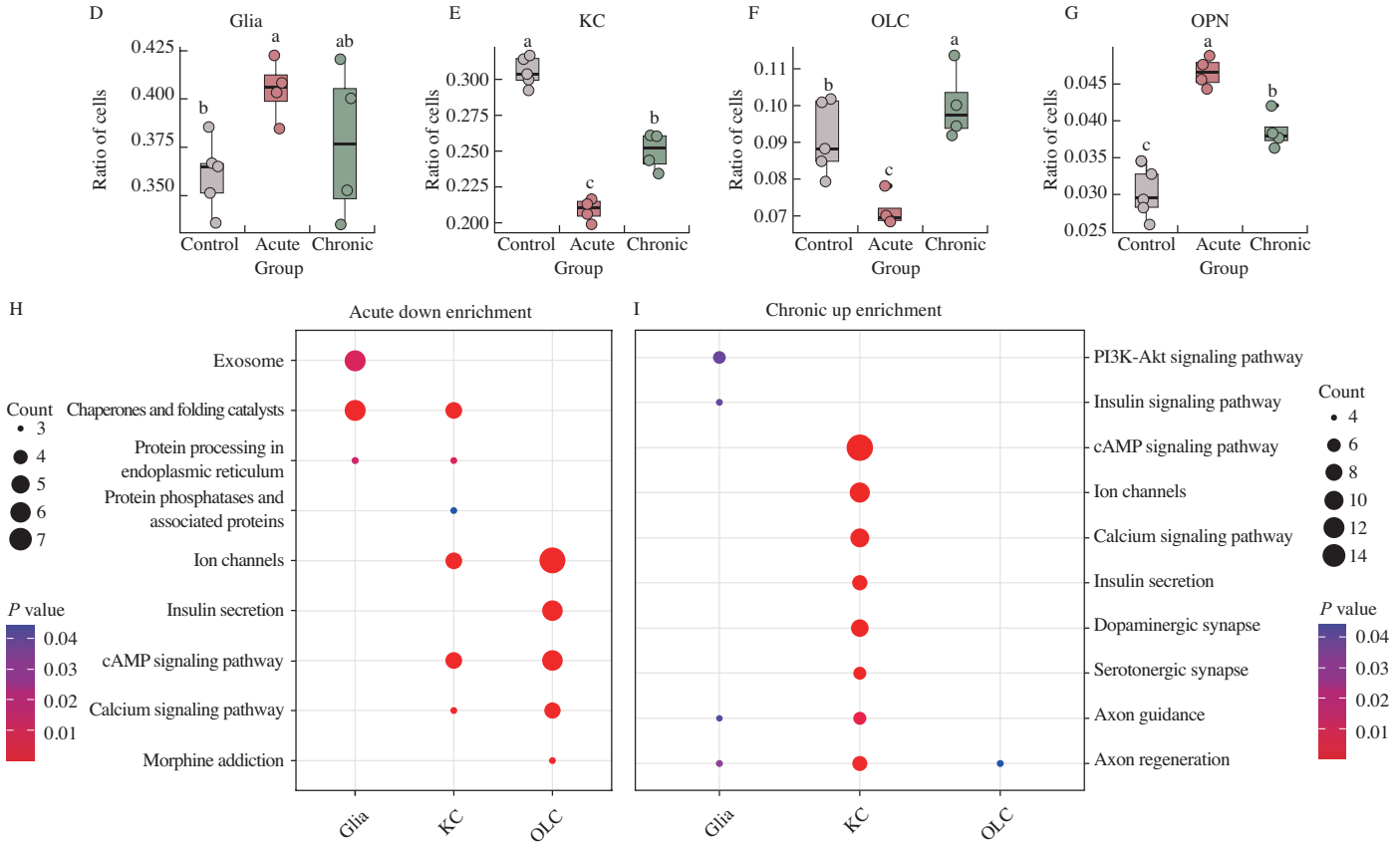

Fig. 2 (*Continued*)

3.3 Acute AA impairs protein synthesis, autophagy, and apoptosis in Glia

We extracted the Glia data and clustered them unsupervised into 10 distinct clusters across all samples (Fig. 3A). Based on the expression of known marker genes, we further divided the Glia into astrocytes (AST; labeled by *Act79B*, *aay*), ensheathing glia (ENS; CG7509, *Tsf1*), cortex glia (COR; *zyd*), perineurial glia (PER; *gem*) and subperineurial glia (subPER; CG9512) (Fig. 3A and Fig. S3A). When comparing the proportions of these cell subtypes under AA exposure, we observed significant changes in AST and PER (Fig. 3B and Fig. S4A). Further DEGs and KEGG enrichment analysis showed that the genes significantly downregulated by acute AA were enriched in pathways such as protein processing in the endoplasmic reticulum and protein phosphatases and associated proteins (Figs. 3C-D). The endoplasmic reticulum is responsible for intricate processes like protein folding and post-translational modifications, including glycosylation and disulfide bond formation, and the downregulation of these pathways means that the normal physiological processes of Glia are disrupted.

To further investigate the effects of acute AA exposure on cellular function, we analyzed DEGs involved in protein-related pathways, including exosome, ribosome, chaperones and folding catalysts, and protein processing in the endoplasmic reticulum. In our data, heat shock proteins, including *Hsp10*, *Hsp60*, *Hsp70*, *Hsp83,* and *L(2) EFL* (LOC100652068) were significantly downregulated in Glia (Figs. 3E-F). These genes play a critical role in preventing preventing protein aggregation and facilitating refolding, thereby maintaining proper protein structure and cellular homeostasis[58]. Among them, heat shock proteins (HSPs) have been widely recognized for their neuroprotective functions in many acute and chronic pathological conditions affecting the brain. In ischemic brain tissue, the protein levels of HSPB1 is specifically increased in AST[59], while overexpression of either HSPA1 or HSPB1 in Alzheimer's disease (AD) mouse has been shown to reduce amyloid beta (Aβ) plaque formation and mitigate cognitive dysfunction[60]. Similarly, in bumblebees we observed that HSP expression was reduced in the Glia of bumblebee brains, which was consistent with behavioral phenotypes observed in bumblebees, including slowed movement and cognitive deficits (Figs. 1B-E and Figs. 3E-F).

RPLP2 (LOC100645225) encodes an acidic ribosomal protein that facilitates the recruitment of translation factors and other ribosomal proteins to the ribosomal complex, thereby promoting protein synthesis (Figs. 3E-F)[61-62]. The ribosomal P complex, composed of acidic ribosomal P (RPLP0, RPLP1, and RPLP2), is crucial in recruiting translation factors and promoting protein synthesis. Reduced expression of RPLP leads to the accumulation of reactive oxygen species, activation of the mitogen-activated protein kinase 1/extracellular signal-regulated kinase 2 (MAPK1/ERK2) signaling pathway, cell cycle arrest, and induction of autophagy[63]. Additionally, acute AA exposure results in the downregulation of the gene that inhibits autophagy (*FKBP4*) (Figs. 3E-F). FKBP4, a member of the pro-immune protein family, plays a multifaceted role in immune regulation and fundamental cellular processes, including protein folding and transport. Overexpression of FKBP4 is associated with increased cell proliferation and inhibition of

apoptosis and autophagy[64-65]. Furthermore, the gene encoding regucalcin (*RGN*), a novel calcium-binding protein, was found to be downregulated (Figs. 3E-F). RGN plays a crucial role in intracellular signaling within both the cytoplasm and nucleus[66]. It has been shown to inhibit cell death and apoptosis triggered by tumor necrosis factor-α or the endoplasmic reticulum Ca^{2+}-ATPase inhibitor thapsigargin. This protective effect is particularly evident against apoptosis induced by lipopolysaccharide and various intracellular signaling-related factors[67]. Therefore, these genes were significantly downregulated after acute AA treatment, implying that the balance between protein synthesis and degradation was disrupted. This disorder inhibits the ability of the endoplasmic reticulum to synthesize proteins normally, disrupting protein homeostasis, autophagy, and apoptosis-related processes in Glia. Autophagy is a process of degradation and recycling of intracellular components that enables cells to capture and degrade their cytoplasm and organelles, which are then consumed in lysosomes, thereby maintaining the stability of the intracellular environment[68]. Dysregulation of autophagy has been implicated in various brain disorders, including AD and Parkinson's disease[69-70]. Specifically, knockdown of autophagy-related components in AST has been shown to result in significant increases in Aβ plaque size and severe cognitive impairments were observed in mouse brains[71]. Moreover, apoptosis, a well-characterized form of programmed cell death, also plays a crucial role in the pathogenesis of neurodegenerative diseases. Wang et al.[72] demonstrated that AA was able to exacerbate apoptosis in HepG2 cells. Similarly, exposure to AA in *D. melanogaster* has been shown to reduce the expression of anti-apoptotic proteins and significantly increase pro-apoptotic proteins, which corresponded with a marked reduction in both survival rate and locomotor activity[73]. Consistent with these findings, acute AA treatment of bumblebees led to a significant decrease in cognitive function, accompanied by significant downregulation of autophagy- and apoptosis-related genes in Glia (Figs. 3E-F).

In conclusion, acute AA exposure may impair the neurological function of bumblebees by disrupting protein homeostasis, autophagy, and apoptosis in Glia, leading to reduced locomotor function and cognitive deficits in the bumblebees' behavior (Fig. 3G).

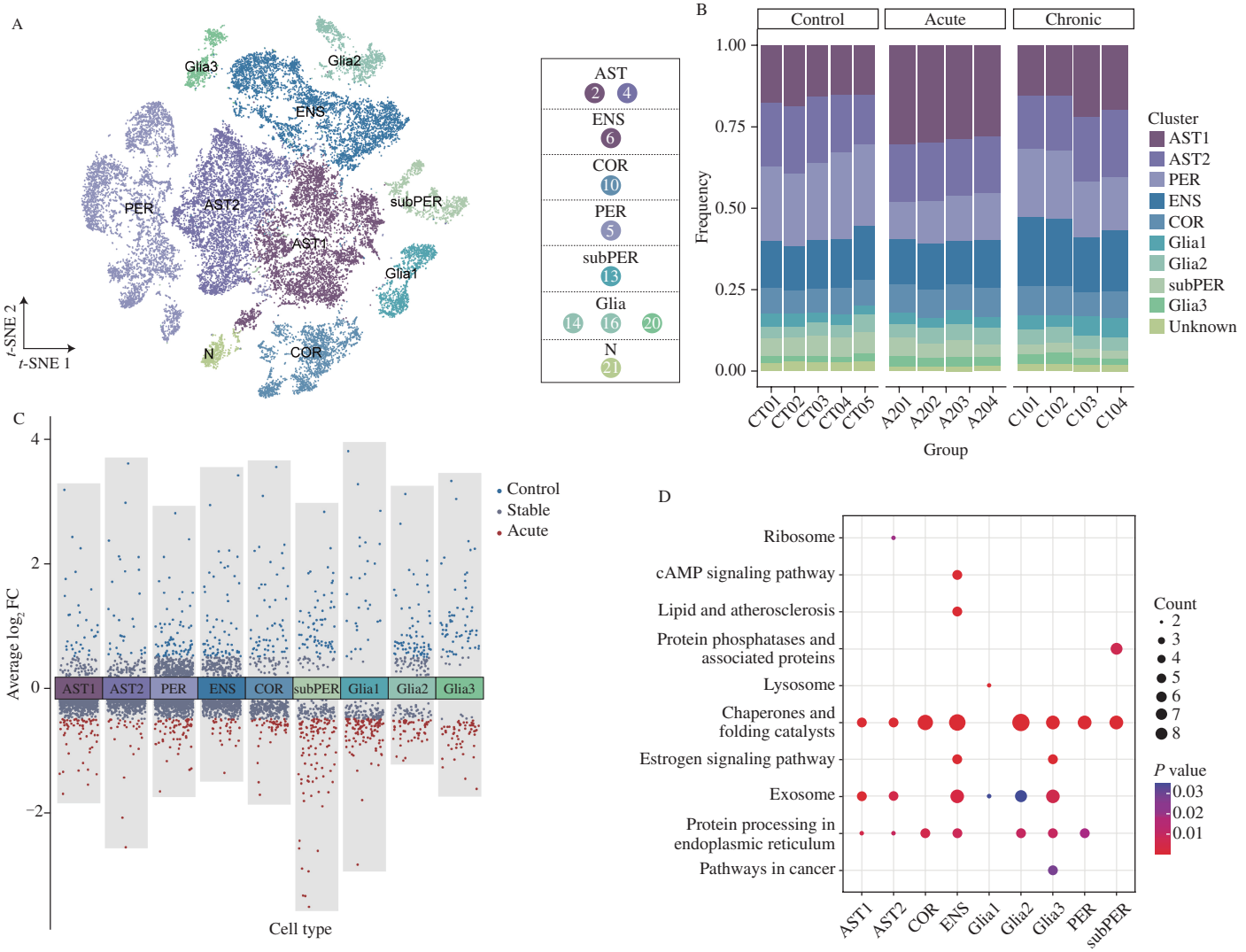

Fig. 3 Glia subtypes' transcriptome responses to AA exposure. (A) *t*-SNE visualization for the Glia subtypes, N is represent for unknown. (B) The proportion of Glia subtypes in control and AA treatment group. (C) DEGs in different Glia subtypes between control and acute AA treatment. (D) Enrichment of DEGs in Glia subtypes between control and acute AA treatment. (E) Heatmap showing the average expression of pathway-enriched genes in Glia subtypes. (F) mRNA levels of *RPLP2*, *Hsp83*, *L(2)EFL*, *FKBP4*, and *RGN* in the brain of bumblebees after exposure to acute AA. (G) Chronic AA inhibits endoplasmic reticulum protein synthesis and induces down-regulation of apoptosis inhibiting genes in Glia, disrupting cell structure and function. Significant differences from the control are indicated by *, ***, $P < 0.05$, $P < 0.001$.

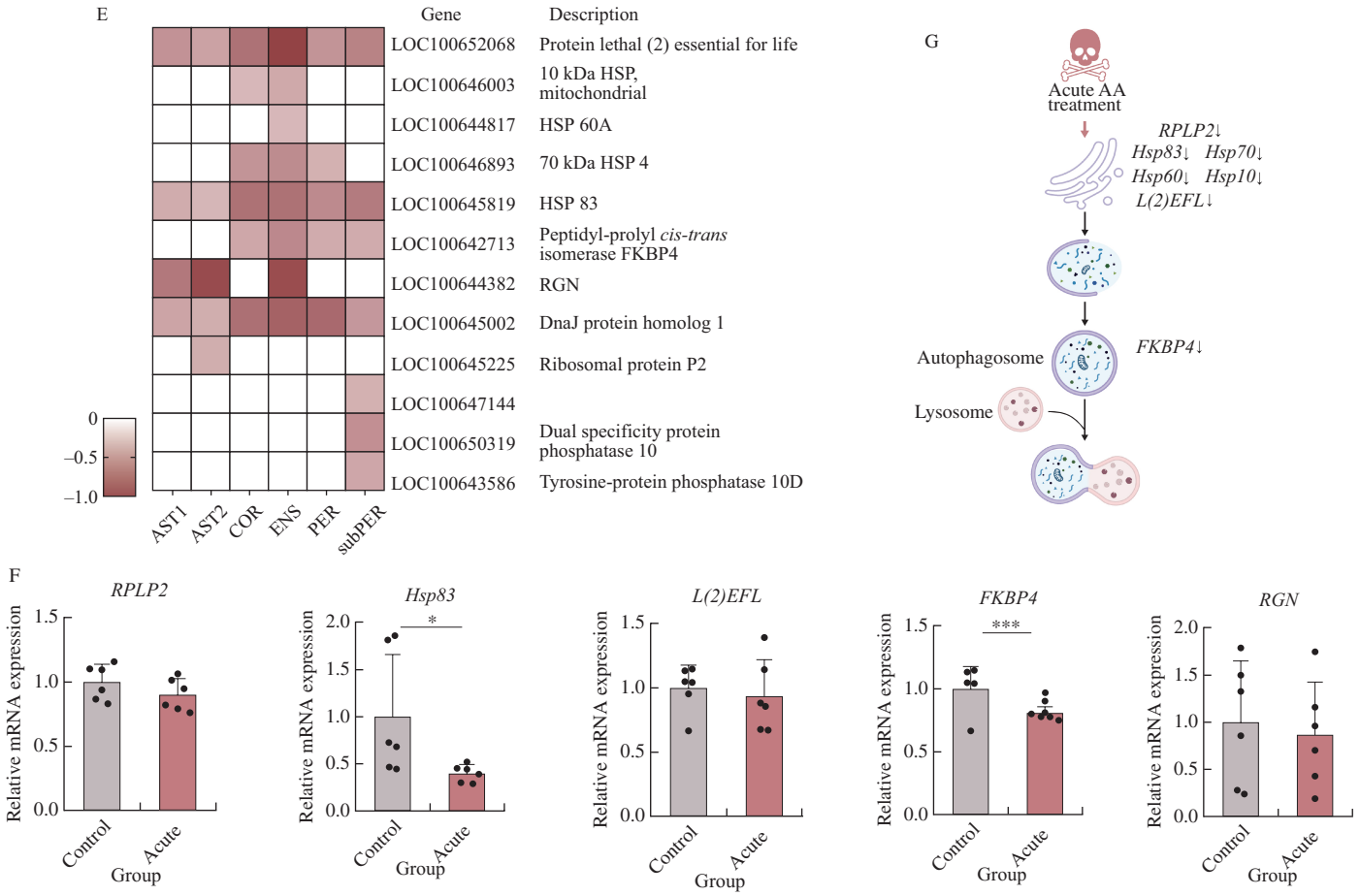

Fig. 3 (*Continued*)

3.4 Chronic AA disrupted intracellular transport in KCs

To further explore the effects of chronic AA on KC, we identified a total of 19 323 individual KC nuclei, which were classified into 7 distinct subgroups based on their unique gene expression profiles. Based on previous morphology and gene expression data, we divided the 7 clusters into 4 subtypes, including class I large-type Kenyon cells (IKCs; characterized by the expression of *Camkii* and *Br-c*), class I medium-type Kenyon cells (mKCs; LOC725542), class I small-type Kenyon cells (sKCs; *Fstl5*), and class II Kenyon cells (IIKCs, LOC408525) (Fig. 4A and Fig. S3B)[74].

We found that the proportion of IKCs and IIKCs changed significantly after chronic AA treatment (Fig. 4B and Fig. S4B). Moreover, we looked into the DEGs and found a total of 2 371 genes distributed among the different KCs subtypes (Fig. 4C). The number of DEGs in IKC and IIKC was 837 and 857, respectively, representing the majority of the total number of DEGs. As intrinsic neurons of insect mushroom bodies, KCs play a pivotal role in learning, memory, and sensory integration[75-76]. Among them, five proteins involved in the intracellular Ca^{2+} signaling pathway, such as Ca^{2+}/calmodulin-dependent protein kinase II (*CaMKII*, LOC100648089), are preferentially expressed in IKCs and are essential for learning and memory[57,77]. The KEGG enrichment results of DEGs demonstrated that biological processes such as cAMP signaling pathway, calcium signaling pathway and ion channels exhibited notable increases in activity following chronic AA treatment (Fig. 4D). Building on the findings from chronic AA treatment, we further analyzed the DEGs within these pathway to investigate whether chronic AA treatment elicited distinct effects compared to acute exposure.

In cells, intracecellular second messengers such as cAMP, Ca^{2+} and other small molecules convert extracellular signals received by cell surface receptors to intracellular signals, thereby regulating inflammation, depression, and learning and memory disorders[78]. In our study, we observed the upregulation of the *Galphas* and *Pka-C1*, which are key components of the cAMP signaling pathway. *Galphas* encodes the G protein alpha s subunit, which activates adenylate cyclase, leading to increased cAMP levels and subsequent activation of protein kinase A (PKA), with *Pka-C1* encoding the catalytic subunit of PKA[79]. Activated PKA phosphorylates target proteins involved in neuronal function. For example, in *Drosophila*, PKA phosphorylates the cyclic AMP response element-binding protein (CREB) transcription factor in the mushroom bodies, playing a key role in long-term memory[80]. These processes may help explain the learning and memory impairments observed in bumblebees after chronic AA treatment (Figs. 1D-E). Moreover, our analysis revealed that genes associated with Ca^{2+}, including *PMCA* and *CaMKII*, are also enriched within the cAMP signaling pathway, calcium signaling pathways and ion channels. It has been demonstrated that following exposure to AA, the basal level of Ca^{2+} concentration in SH-SY5Y cells exhibited a 49% increase[81]. Interestingly, after chronic AA treatment, we found that the expression of plasma membrane Ca^{2+} ATPase (*PMCA*, LOC100645179) was upregulated in KC (Figs. 4E-F),

which is a high-affinity calcium pump responsible for transporting Ca^{2+} into the extracellular space and maintaining calcium homeostasis between the cytoplasm and the extracellular environment[82]. Given that Ca^{2+} plays a role in the release of synaptic vesicles, and the fundamental basis of learning and memory in synaptic activity[83], we postulated that chronic AA exposure may impair learning and cognitive behavior by increasing Ca^{2+} concentrations in neurons. Additionally, the expression of *CaMKII* was observed to have increased (Fig. 4E). Finally, qPCR analysis showed a upward trend in gene expression, in agreement with the snRNA-seq results, but did not reach statistical significance (Fig. 4F), likely because KC-specific transcriptional changes were masked by averaged expression across cell populations. CaMKII is a protein kinase regulated by the Ca^{2+}/calmodulin complex, in neurons, as Ca^{2+} and calmodulin accumulate, CaMKII undergoes autophosphorylation, causing CaMKII to be continuously activated for a short period, and regulate long-term potentiation in cells, which is considered to be the basis of the memory process[84]. Nevertheless, excessive CAMKII autophosphorylation may result in the transcription of hyperphosphorylated Tau protein, thereby contributing to neuronal damage and the development of neurological disorders[85]. Moreover, the expression of *CACNB2* (LOC100645652) was elevated (Figs. 4E-F), which is responsible for encoding the voltage-dependent *L*-type calcium channel subunit beta-2 ($Ca_V\beta_2$). $Ca_V\beta_2$ are responsible for regulating the trafficking of the respective Ca^{2+} channel to the plasma membrane, and they are also involved in the modulation of gating properties[86]. It has been demonstrated that *CACNB2* is a prevalent risk gene for mental illness, with a correlation observed between its presence and the development of conditions such as schizophrenia and AD[87]. Interestingly, CaMKII can phosphorylate $Ca_V\beta$, thereby playing a role in the facilitation of *L*-type Ca^{2+} channels[86]. In conclusion, it can be postulated that chronic AA may impair learning and memory by upregulating Ca^{2+} in KCs and disrupting synaptic activities, including intracellular Ca^{2+} transport and CaMKII phosphorylation.

Other than disruption in calcium signaling, KEGG enrichment analysis also showed the upregulation of axon transport induced by chronic AA, such as axon guidance and axon regeneration pathways (Fig. 4D). Axons house over 99% of neuronal cytoplasm to translocate nutrients and waste products within the cell, primarily through active transport[88]. Specifically, chronic AA treatment resulted in the upregulation of two genes, namely *DYNC1H1* (LOC100647009) and *KIF21A* (LOC100649572) (Figs. 4E-F), which encode for cytoplasmic dynein heavy chain 1 and kinesin family member 21A, respectively. Similarly, *in vitro* cell experiments, chronic AA treatment significantly increased the levels of kinesin and dynein proteins[89]. Both dynein and kinesin are motor proteins involved in intracellular transport. Kinesin is typically the anterograde motor protein that facilitates the transport of cargoes towards the synapse, whereas dynein is regarded as the retrograde motor protein that enables the transportation of cargoes towards the cell body, and abnormal amounts of either motor protein can impair axonal transport in both anterograde and antidromic directions[89-92]. Dysfunction in axonal transport has been associated with various neurodegenerative diseases, including AD[93]. Given this association, we postulate that axonal transport disorders may also contribute to impaired learning and memory.

In summary, chronic AA primarily impacts KCs by altering intracellular calcium concentrations, which, in turn, disrupts cellular metabolism, ultimately leading to damage in the CNS. Furthermore, the upregulation of kinesin and dynein genes by AA may affect intracellular trafficking, leading to the development of neurodegenerative diseases (Fig. 4G).

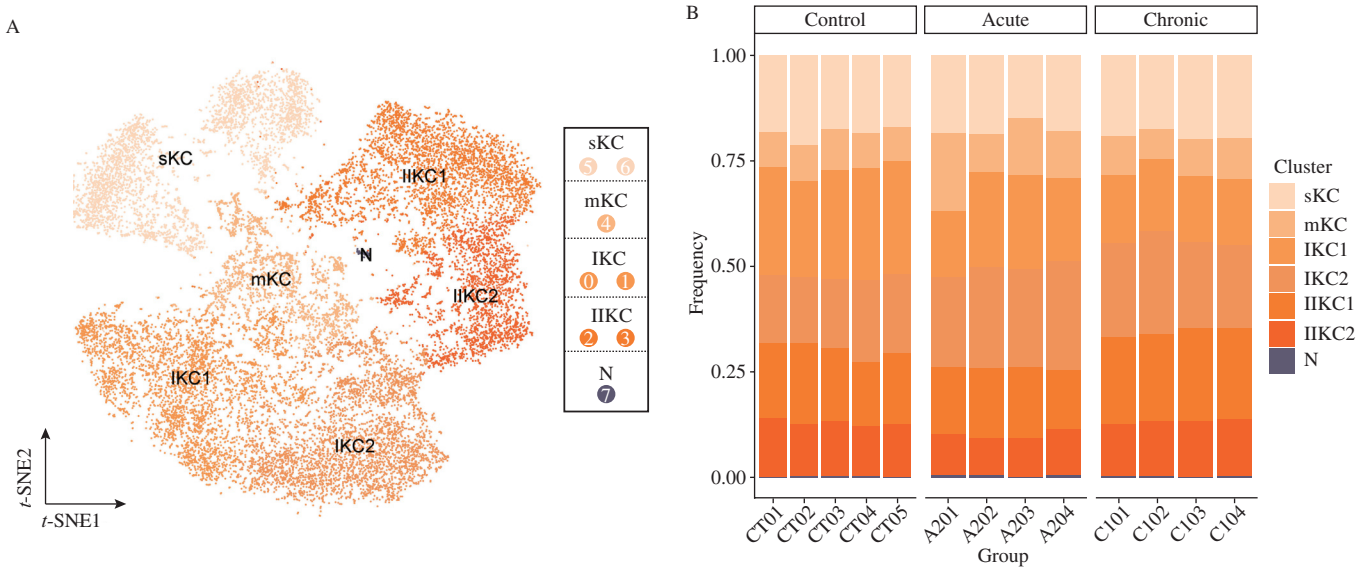

Fig. 4 KC subtypes' transcriptome responses to chronic AA exposure. (A) *t*-SNE visualization of KC subclusters. (B) The proportion of KC subtypes in control and AA treatment group. (C) DEGs in different KC subtypes between control and chronic AA treatment. (D) Enrichment of DEGs in KC subtypes between control and chronic AA treatment. (E) Heatmap showing DEGs after chronic AA exposure. Potential mechanism of chronic AA in KCs.(F) mRNA levels of *DYNC1H1*, *KIF21A*, *PMCA*, *CaMKII*, and *CACNB2* in the brain of bumblebees after exposure to chronic AA. (G) Potential mechanism of chronic AA in KCs. Significant differences from the control are indicated by *, $P < 0.05$.

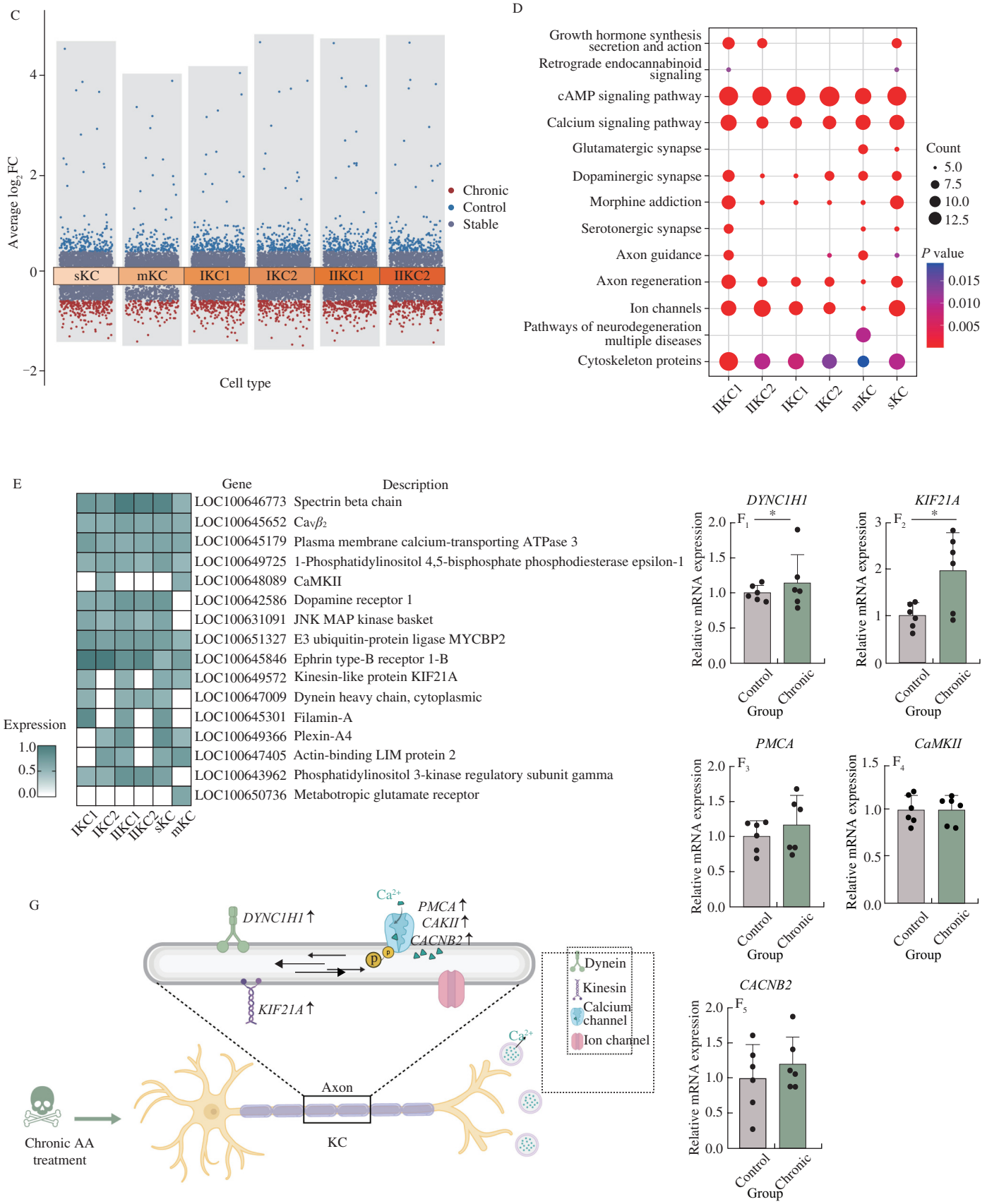

Fig. 4 (*Continued*)

4. Conclusion

AA has long been linked to carcinogenic and neurotoxic effects through multiple signaling pathways, but the precise mechanism remains unclear. In this study, we employed bumblebees as a model organism to investigate the underlying mechanisms of acute and chronic AA. Following exposure to AA, the survival rate of bumblebees declined significantly, accompanied by a considerable reduction in mobility, learning, and memory abilities. SnRNA-seq revealed that AA exposure did not change the cell type clustering outcomes, however, acute and chronic AA-induced cell-specific responses. Specifically, acute AA exposure impaired protein synthesis, autophagy, and apoptosis in Glia, while chronic AA exposure primarily disrupted the axon transport and the equilibrium of Ca^{2+} in KC. These cellular changes were associated with behavioral deficits in bumblebees, including slowed movement and cognitive impairment. Although the doses and experimental protocols in this study were designed to reflect human intake levels and those commonly used in mouse, fruit fly, and cell-based experiments, the direct applicability of these findings to human mechanisms remains uncertain. Therefore, further clinical and epidemiological studies are required in the future to enhance the understanding of the mechanism of action of AA on the CNS under diverse circumstances.

Declaration of competing interest

Hao Zheng is an editorial board member for *Food Science and Human Wellness* and was not involved in the editorial review or the decision to publish this article. The authors declare that they have no known competing financial interests or personal relationships that could have appeared to influence the work reported in this paper.

Acknowledgements

This work was supported by the National Natural Science Foundation of China Project (32230081).

Research ethics approval

This work has received approval for research ethics from China Agricultural University (20220621-3).

Data availability

The raw data of the snRNA-seq have been deposited into the CNGB Sequence Archive[94] of China National GeneBank DataBase[95] with accession numbers CNPO004450.

Appendix A. Supplementary data

Supplementary data associated with this article can be found, in the online version, at http://doi.org/10.26599/FSHW.2024.9250457.

References

[1] M. Zhao, B. Zhang, L. Deng, The mechanism of acrylamide-induced neurotoxicity: current status and future perspectives, Front. Nutr. 9 (2022) 859189. https://doi.org/10.3389/fnut.2022.859189.

[2] D.S. Mottram, B.L. Wedzicha, A.T. Dodson, Acrylamide is formed in the Maillard reaction, Nature 419 (2002) 448-449. https://doi.org/10.1038/419448a.

[3] R.H. Stadler, I. Blank, N. Varga, et al., Acrylamide from Maillard reaction products, Nature 419 (2002) 449-450. https://doi.org/10.1038/419449a.

[4] L.A. Mucci, K.M. Wilson, Acrylamide intake through diet and human cancer risk, J. Agric. Food Chem. 56 (2008) 6013-6019. https://doi.org/10.1021/jf703747b.

[5] M. Huang, J. Jiao, J. Wang, et al., Characterization of acrylamide-induced oxidative stress and cardiovascular toxicity in zebrafish embryos, J. Hazard. Mater. 347 (2018) 451-460. https://doi.org/10.1016/j.jhazmat.2018.01.016.

[6] S. Senthilkumar, R. Raveendran, S. Madhusoodanan, et al., Developmental and behavioural toxicity induced by acrylamide exposure and amelioration using phytochemicals in *Drosophila melanogaster*, J. Hazard. Mater. 394 (2020) 122533. https://doi.org/10.1016/j.jhazmat.2020.122533

[7] H. Wang, P. Huang, T. Lie, et al., Reproductive toxicity of acrylamide-treated male rats, Reprod. Toxicol. 29 (2010) 225-230. https://doi.org/10.1016/j.reprotox.2009.11.002.

[8] D. Yu, Q. Liu, B. Qiao, et al., Exposure to acrylamide inhibits uterine decidualization via suppression of cyclin D3/p21 and apoptosis in mice, J. Hazard. Mater. 388 (2020) 121785. https://doi.org/10.1016/j.jhazmat.2019.121785.

[9] Y. Komoike, M. Matsuoka, *In vitro* and *in vivo* studies of oxidative stress responses against acrylamide toxicity in zebrafish, J. Hazard. Mater. 365 (2019) 430-439. https://doi.org/10.1016/j.jhazmat.2018.11.023.

[10] M.K. Virk-Baker, T.R. Nagy, S. Barnes, et al., Dietary acrylamide and human cancer: a systematic review of literature, Nutr, Cancer. 66 (2014) 774-790. https://doi.org/10.1080/01635581.2014.916323.

[11] J.E. Klaunig, Acrylamide carcinogenicity, J. Agric. Food Chem. 56 (2008) 5984-5988. https://doi.org/10.1021/jf8004492.

[12] N. Mei, L.P. McDaniel, V.N. Dobrovolsky, et al., The genotoxicity of acrylamide and glycidamide in big blue rats, Toxicol. Sci. 115 (2010) 412-421. https://doi.org/10.1093/toxsci/kfq069.

[13] A.S. Kuperman, Effects of acrylamide on the central nervous system of the cat, J. Pharmacol. Exp. Ther. 123 (1958) 180-192. https://doi.org/10.1016/S0022-3565(25)12490-7.

[14] F.S. He, S.L. Zhang, H.L. Wang, et al., Neurological and electroneuromyographic assessment of the adverse effects of acrylamide on occupationally exposed workers, Scand. J. Work Environ. Health 15 (1989) 125-129. https://doi.org/10.5271/sjweh.1878.

[15] Evaluation of certain contaminants in food, WHO TRS. (2017) 1-166.

[16] R.M. LoPachin Jr., E.J. Lehning, Acrylamide-induced distal axon degeneration: a proposed mechanism of action, Neurotoxicology 15 (1994) 247-259.

[17] B. Liang, Y. Huang, Y. Zhong, et al., Brain single-nucleus transcriptomics highlights that polystyrene nanoplastics potentially induce Parkinson's disease-like neurodegeneration by causing energy metabolism disorders in mice, J. Hazard. Mater. 430 (2022) 128459. https://doi.org/10.1016/j.jhazmat.2022.128459.

[18] M.T. Dang, F. Mafra, M. Haldar, Isolation of myeloid cells from mouse brain tumors for single-cell RNA-seq analysis, Star. Protoc. 2 (2021) 100957. https://doi.org/10.1016/j.xpro.2021.100957.

[19] N.S. Michki, Y. Li, K. Sanjasaz, et al., The molecular landscape of neural differentiation in the developing *Drosophila* brain revealed by targeted scRNA-seq and multi-informatic analysis, Cell Rep. 35 (2021) 109039. https://doi.org/10.1016/j.celrep.2021.109039.

[20] Y. Tian, M.Y. Zhang, A.H. Zhao, et al., Single-cell transcriptomic profiling provides insights into the toxic effects of Zearalenone exposure on primordial follicle assembly, Theranostics 11 (2021) 5197-5213. https://doi.org/10.7150/thno.58433.

[21] A. Martin, A. Babbitt, A.G. Pickens, et al., Single-cell RNA sequencing characterizes the Molecular Heterogeneity of the larval zebrafish optic tectum, Front. Mol. Neurosci. 15 (2022) 818007. https://doi.org/10.3389/fnmol.2022.818007.

[22] J. Yu, W. Cheng, M. Jia, et al., Toxicity of perfluorooctanoic acid on zebrafish early embryonic development determined by single-cell RNA sequencing, J. Hazard. Mater. 427 (2022) 127888. https://doi.org/10.1016/j.jhazmat.2021.127888.

[23] M.N.H. Khabib, Y. Sivasanku, H.B. Lee, et al., Alternative animal models in predictive toxicology, Toxicology 465 (2022) 153053. https://doi.org/10.1016/j.tox.2021.153053

[24] X.C. Fei, C. Song, H.W. Gao, Transmembrane transports of acrylamide and bisphenol A and effects on development of zebrafish (*Danio rerio*), J. Hazard. Mater. 184 (2010) 81-88. https://doi.org/10.1016/j.jhazmat.2010.08.007.

[25] R.L. Kachot, U.D. Patel, H.B. Patel, et al., Neurotoxicity of acrylamide in adult zebrafish following short-term and long-term exposure: evaluation of behavior alterations, oxidative stress markers, expression of antioxidant genes, and histological examination of the brain and eyes, Environ. Sci. Pollut. Res. 30 (2023) 40116-40131. https://doi.org/10.1007/s11356-022-25112-z.

[26] S.M. Murray, B.M. Waddell, C.W. Wu, Neuron-specific toxicity of chronic acrylamide exposure in *C. elegans*, Neurotoxicol Teratol. 77 (2020) 106848. https://doi.org/10.1016/j.ntt.2019.106848.

[27] L. Li, H. Maboudi, M. Egertová, et al., A possible structural correlate of learning performance on a colour discrimination task in the brain of the bumblebee, Proc. R. Soc. B: Biol. Sci. 284 (2017) 20171323. https://doi.org/10.1098/rspb.2017.1323.

[28] K. Beer, E. Kolbe, N.B. Kahana, et al., Pigment-dispersing factor-expressing neurons convey circadian information in the honey bee brain, Open Biol. 8 (2018). https://doi.org/10.1098/rsob.170224.

[29] L. Li, S. Su, C.J. Perry, et al., Large-scale transcriptome changes in the process of long-term visual memory formation in the bumblebee, *Bombus terrestris*, Sci. Rep. 8 (2018) 534. https://doi.org/10.1038/s41598-017-18836-3.

[30] J. Chen, X. Mu, H. Liu, et al., Rotenone impairs brain glial energetics and locomotor behavior in bumblebees, Sci. Total Environ. 907 (2024) 167870. https://doi.org/10.1016/j.scitotenv.2023.167870.

[31] A. Dobin, C.A. Davis, F. Schlesinger, et al., STAR: ultrafast universal RNA-seq aligner, Bioinformatics 29 (2013) 15-21. https://doi.org/10.1093/bioinformatics/bts635.

[32] A. Tarasov, A.J. Vilella, E. Cuppen, et al., Sambamba: fast processing of NGS alignment formats, Bioinformatics 31 (2015) 2032-2034. https://doi.org/10.1093/bioinformatics/btv098.

[33] M.D. Young, S. Behjati, SoupX removes ambient RNA contamination from droplet-based single-cell RNA sequencing data, GigaScience 9 (2020) giaa151. https://doi.org/10.1093/gigascience/giaa151.

[34] W. Zhang, L. Wang, Y. Zhao, et al., Single-cell transcriptomic analysis of honeybee brains identifies vitellogenin as caste differentiation-related factor, iScience 25 (2022) 104643. https://doi.org/10.1016/j.isci.2022.104643.

[35] K. Davie, J. Janssens, D. Koldere, et al., A single-cell transcriptome atlas of the aging *Drosophila* brain, Cell. 174 (2018) 982-998. e920. https://doi.org/10.1016/j.cell.2018.05.057.

[36] L. Sheng, E.J. Shields, J. Gospocic, et al., Social reprogramming in ants induces longevity-associated glia remodeling, Sci. Adv. 6 (2020) eaba9869. https://doi.org/10.1126/sciadv.aba9869.

[37] Q. Li, M. Wang, P. Zhang, et al., A single-cell transcriptomic atlas tracking the neural basis of division of labour in an ant superorganism, Nat. Ecol. Evol. 6 (2022) 1191-1204. https://doi.org/10.1038/s41559-022-01784-1.

[38] E. Prats, C. Gómez-Canela, S. Ben-Lulu, et al., Modelling acrylamide acute neurotoxicity in zebrafish larvae, Sci. Rep. 7 (2017) 13952. https://doi.org/10.1038/s41598-017-14460-3.

[39] J. Manson, M.J. Brabec, J. Buelke-Sam, et al., NTP-CERHR expert panel report on the reproductive and developmental toxicity of acrylamide, Birth Defects Res. B Dev. Reprod. Toxicol. 74 (2005) 17-113. https://doi.org/10.1002/bdrb.20030.

[40] A. Koszucka, A. Nowak, I. Nowak, et al., Acrylamide in human diet, its metabolism, toxicity, inactivation and the associated European Union legal regulations in food industry, Crit. Rev Food Sci. Nutr. 60 (2020) 1677-1692. https://doi.org/10.1080/10408398.2019.1588222.

[41] M. Faria, T. Ziv, C. Gómez-Canela, et al., Acrylamide acute neurotoxicity in adult zebrafish, Sci. Rep. 8 (2018) 7918. https://doi.org/10.1038/s41598-018-26343-2.

[42] X. Yao, L. Yan, L. Yao, et al., Acrylamide exposure impairs blood-cerebrospinal fluid barrier function, Neural Regen. Res. 9 (2014) 555-560. https://doi.org/10.4103/1673-5374.130080.

[43] P. Schneider, Y.J. Ho, R. Spanagel, et al., A novel elevated plus-maze procedure to avoid the one-trial tolerance problem, Front. Behav. Neurosci. 5 (2011) 43. https://doi.org/10.3389/fnbeh.2011.00043.

[44] R.M. LoPachin, T. Gavin, Molecular mechanism of acrylamide neurotoxicity: lessons learned from organic chemistry, Environ. Health Perspect. 120 (2012) 1650-1657. https://doi.org/10.1289/ehp.1205432.

[45] M.M. Üremiş, N. Üremiş, M. Gül, et al., Acrylamide, applied during pregnancy and postpartum period in offspring rats, significantly disrupted myelination by decreasing the levels of myelin-related proteins: MBP, MAG, and MOG, Neurochem. Res. 49 (2024) 617-635. https://doi.org/10.1007/s11064-023-04053-0.

L. Li, J. Li, L. Luo, et al., Toxic encephalopathy, vision loss, and memory disorder caused by acute acrylamide exposure, J. Occup. Environ. Hyg. 21 (2024) 152-161. https://doi.org/10.1080/15459624.2024.2305135.

[47] J.S. Park, P. Samanta, S. Lee, et al., Developmental and neurotoxicity of acrylamide to zebrafish, Int. J. Mol. Sci. 22 (2021) 3518. https://doi.org/10.3390/ijms22073518.

[48] Z. Tandisehpanah, A. Foroutanfar, A. Aziminia, et al., Protective effect of aqueous and ethanolic extracts of *Lippia citriodora* Kunth. on acrylamide-induced neurotoxicity, Avicenna J. Phytomed. 12 (2022) 281-294. https://doi.org/10.22038/ajp.2021.19173.

[49] W. Quan, M. Li, Y. Jiao, et al., Effect of dietary exposure to acrylamide on diabetes-associated cognitive dysfunction from the perspectives of oxidative damage, neuroinflammation, and metabolic disorders, J. Agric. Food Chem. 70 (2022) 4445-4456. https://doi.org/10.1021/acs.jafc.2c00662.

[50] F. Hosseini-Esfahani, N. Beheshti, A. Nematollahi, et al., The association between dietary acrylamide intake and the risk of type 2 diabetes incidence in the Tehran lipid and glucose study, Sci. Rep. 13 (2023) 8235. https://doi.org/10.1038/s41598-023-35493-x.

[51] A. Zayed, G.E. Robinson, Understanding the relationship between brain gene expression and social behavior: lessons from the honey bee, Annu. Rev. Genet. 46 (2012) 591-615. https://doi.org/10.1146/annurev-genet-110711-155517.

[52] P. Schotman, L. Gipon, F.G. Jennekens, et al., Polyneuropathies and CNS protein metabolism. III. Changes in protein synthesis rate induced by acrylamide intoxication, J. Neuropathol. Exp. Neurol. 37 (1978) 820-837.

[53] P. Schotman, L. Gipon, F. Jennekens, et al., Polyneuropathies and CNS protein metabolism. II. Changes in the incorporation rate of leucine during acrylamide intoxication, Neuropathol. Appl. Neurobiol. 3 (1977) 125-136.

[54] N.J. Allen, D.A. Lyons, Glia as architects of central nervous system formation and function, Science 362 (2018) 181-185. https://doi.org/10.1126/science.aat0473.

[55] R. Von Burg, D. Penney, P. Conroy, Acrylamide neurotoxicity in the mouse: a behavioral, electrophysiological and morphological study, J. Appl. Toxicol. 1 (1981) 227-233.

[56] G. Song, Z. Liu, L. Wang, et al., Protective effects of lipoic acid against acrylamide-induced neurotoxicity: involvement of mitochondrial energy metabolism and autophagy, Food Funct. 8 (2017) 4657-4667. https://doi.org/10.1039/c7fo01429e.

[57] S. Suenami, S. Oya, H. Kohno, et al., Kenyon cell subtypes/populations in the honeybee mushroom bodies: possible function based on their gene expression profiles, differentiation, possible evolution, and application of genome editing, Front. Psychol. 9 (2018) 1717. https://doi.org/10.3389/fpsyg.2018.01717.

[58] L. Böttinger, S. Oeljeklaus, B. Guiard, et al., Mitochondrial heat shock protein (Hsp) 70 and Hsp10 cooperate in the formation of Hsp60 complexes, J. Biol. Chem. 290 (2015) 11611-11622. https://doi.org/10.1074/jbc.M115.642017.

[59] F.R. Sharp, X. Zhan, D.Z. Liu, Heat shock proteins in the brain: role of Hsp70, Hsp27, and HO-1 (Hsp32) and their therapeutic potential, Transl. Stroke Res. 4 (2013) 685-692. https://doi.org/10.1007/s12975-013-0271-4.

[60] T. Hoshino, N. Murao, T. Namba, et al., Suppression of Alzheimer's disease-related phenotypes by expression of heat shock protein 70 in mice, J. Neurophysiol. 31 (2011) 5225-5234. https://doi.org/10.1523/jneurosci.5478-10.2011.

[61] N. Ban, R. Beckmann, J.H. Cate, et al., A new system for naming ribosomal proteins, Curr. Opin. Struct. Biol. 24 (2014) 165-169. https://doi.org/10.1016/j.sbi.2014.01.002.

[62] C.H. Wang, L.K. Wang, C.C. Wu, et al., The ribosomal protein RPLP0 mediates PLAAT4-induced cell cycle arrest and cell apoptosis, Cell Biochem. Biophys. 77 (2019) 253-260. https://doi.org/10.1007/s12013-019-00876-3.

[63] A. Artero-Castro, M. Perez-Alea, A. Feliciano, et al., Disruption of the ribosomal P complex leads to stress-induced autophagy, Autophagy 11 (2015) 1499-1519. https://doi.org/10.1080/15548627.2015.1063764

[64] W. Meng, J. Meng, H. Jiang, et al., FKBP4 accelerates malignant progression of non-small-cell lung cancer by activating the Akt/mTOR signaling pathway, Anal. Cell. Pathol. 2020 (2020) 6021602. https://doi.org/10.1155/2020/6021602.

[65] S. Zong, Y. Jiao, X. Liu, et al., FKBP4 integrates FKBP4/Hsp90/IKK with FKBP4/Hsp70/RelA complex to promote lung adenocarcinoma progression via IKK/NF-κB signaling, Cell Death Dis. 12 (2021) 602. https://doi.org/10.1038/s41419-021-03857-8.

[66] T. Singh, P. Banerjee, Uditi, et al., Expression of regucalcin, a calcium-binding protein is regulated by hypoxia-inducible factor-1α, Life Sci. 292 (2022) 120278. https://doi.org/10.1016/j.lfs.2021.120278.

[67] T. Nakagawa, M. Yamaguchi, Overexpression of regucalcin suppresses apoptotic cell death in cloned normal rat kidney proximal tubular epithelial NRK52E cells: change in apoptosis-related gene expression, J. Cell. Biochem. 96 (2005) 1274-1285. https://doi.org/10.1002/jcb.20617.

[68] J.D. Rabinowitz, E. White, Autophagy and metabolism, Science 330 (2010) 1344-1348. https://doi.org/10.1126/science.1193497.

[69] R.A. Nixon, Autophagy, amyloidogenesis and Alzheimer disease, J. Cell Sci. 120 (2007) 4081-4091. https://doi.org/10.1242/jcs.019265.

[70] L. Nechushtai, D. Frenkel, R. Pinkas-Kramarski, Autophagy in Parkinson's disease, Biomolecules 13 (2023). https://doi.org/10.3390/biom13101435.

[71] S. Kim, H. Chun, Y. Kim, et al., Astrocytic autophagy plasticity modulates Aβ clearance and cognitive function in Alzheimer's disease, Mol. Neurodegener. 19 (2024) 55. https://doi.org/10.1186/s13024-024-00740-w.

[72] A. Wang, X. Chen, L. Wang, et al., Catechins protect against acrylamide- and glycidamide-induced cellular toxicity via rescuing cellular apoptosis and DNA damage, Food Chem. Toxicol. 167 (2022) 113253. https://doi.org/10.1016/j.fct.2022.113253

[73] O.M. Farodoye, T.A. Otenaike, J.S. Loreto, et al., Evidence of acrylamide-induced behavioral deficit, mitochondrial dysfunction and cell death in *Drosophila melanogaster*, Comp. Biochem. Physiol. C 284 (2024) 109971. https://doi.org/10.1016/j.cbpc.2024.109971.

[74] K. Kaneko, S. Suenami, T. Kubo, Gene expression profiles and neural activities of Kenyon cell subtypes in the honeybee brain: identification of novel 'middle-type' Kenyon cells, Zool. Lett. 2 (2016) 14. https://doi.org/10.1186/s40851-016-0051-6.

[75] F. Locatelli, G. Bundrock, U. Müller, Focal and temporal release of glutamate in the mushroom bodies improves olfactory memory in *Apis mellifera*, J. Neurophysiol. 25 (2005) 11614-11618. https://doi.org/10.1523/jneurosci.3180-05.2005.

[76] J. Erber, T. Masuhr, R. Menzel, Localization of short-term memory in the brain of the bee, *Apis mellifera*, Physiol. Entomol. 5 (1980) 343-358.

[77] R.J. Colbran, A.M. Brown, Calcium/calmodulin-dependent protein kinase II and synaptic plasticity, Curr. Opin. Neurobiol. 14 (2004) 318-327. https://doi.org/10.1016/j.conb.2004.05.008.

[78] K. Yan, L.N. Gao, Y.L. Cui, et al., The cyclic AMP signaling pathway: exploring targets for successful drug discovery (Review), Mol. Med. Rep. 13 (2016) 3715-3723. https://doi.org/10.3892/mmr.2016.5005.

[79] M. Zaccolo, A. Zerio, M.J. Lobo, Subcellular organization of the cAMP signaling pathway, Pharmacol. Rev. 73 (2021) 278-309. https://doi.org/10.1124/pharmrev.120.000086.

[80] P.T. Lee, G. Lin, W.W. Lin, et al., A kinase-dependent feedforward loop affects CREBB stability and long term memory formation, eLife 7 (2018). https://doi.org/10.7554/eLife.33007.

[81] M. Nordin-Andersson, E. Walum, P. Kjellstrand, et al., Acrylamide-induced effects on general and neurospecific cellular functions during exposure and recovery, Cell Biol. Toxicol. 19 (2003) 43-51. https://doi.org/10.1023/a:1022017731328.

[82] M. Brini, Plasma membrane Ca^{2+}-ATPase: from a housekeeping function to a versatile signaling role, Pflügers Arch. 457 (2009) 657-664. https://doi.org/10.1007/s00424-008-0505-6.

[83] E. Carafoli, Calcium pump of the plasma membrane, Physiol. Rev. 71 (1991) 129-153. https://doi.org/10.1152/physrev.1991.71.1.129.

[84] W.D. Yao, C.F. Wu, Distinct roles of CaMKII and PKA in regulation of firing patterns and K^+ currents in *Drosophila* neurons, J. Neurophysiol. 85 (2001) 1384-1394. https://doi.org/10.1152/jn.2001.85.4.1384.

[85] A. Ghosh, K.P. Giese, Calcium/calmodulin-dependent kinase II and Alzheimer's disease, Mol Brain 8 (2015) 78. https://doi.org/10.1186/s13041-015-0166-2.

[86] Z. Buraei, J. Yang, The β subunit of voltage-gated Ca^{2+} channels, Physiol. Rev. 90 (2010) 1461-1506. https://doi.org/10.1152/physrev.00057.2009.

[87] A. Andrade, A. Brennecke, S. Mallat, et al., Genetic associations between voltage-gated calcium channels and psychiatric disorders, Int. J. Mol. Sci. 20 (2019) 3537. https://doi.org/10.3390/ijms20143537.

[88] P. Guedes-Dias, E.L.F. Holzbaur, Axonal transport: driving synaptic function, Science. 366 (2019) eaaw9997. https://doi.org/10.1126/science.aaw9997.

[89] L. An, G. Li, J. Si, et al., Acrylamide retards the slow axonal transport of neurofilaments in rat cultured dorsal root ganglia neurons and the corresponding mechanisms, Neurochem. Res. 41 (2016) 1000-1009. https://doi.org/10.1007/s11064-015-1782-z.

[90] A.D. Pilling, D. Horiuchi, C.M. Lively, et al., Kinesin-1 and dynein are the primary motors for fast transport of mitochondria in *Drosophila* motor axons, MBoC. 17 (2006) 2057-2068. https://doi.org/10.1091/mbc.e05-06-0526.

[91] T. Shpilka, C.M. Haynes, The mitochondrial UPR: mechanisms, physiological functions and implications in ageing, Nat. Rev. Mol. Cell Biol. 19 (2018) 109-120. https://doi.org/10.1038/nrm.2017.110.

[92] S.E. Cason, E.L.F. Holzbaur, Selective motor activation in organelle transport along axons, Nat. Rev. Mol. Cell Biol. 23 (2022) 699-714. https://doi.org/10.1038/s41580-022-00491-w.

[93] J.N. Sleigh, A.M. Rossor, A.D. Fellows, et al., Axonal transport and neurological disease, Nat. Rev. Neurol. 15 (2019) 691-703. https://doi.org/10.1038/s41582-019-0257-2.

[94] X. Guo, F. Chen, F. Gao, et al., CNSA: a data repository for archiving omics data, Database (Oxford). 2020 (2020). https://doi.org/10.1093/database/baaa055.

[95] F.Z. Chen, L.J. You, F. Yang, et al., CNGBdb: China National GeneBank DataBase, Yi Chuan 42 (2020) 799-809. https://doi.org/10.16288/j.yczz.20-080.